Mutations in the neutral sphingomyelinase gene *SMPD3* implicate the ceramide pathway in human leukemias

Woo Jae Kim,[1] Ross A. Okimoto,[1] Louise E. Purton,[2] Meagan Goodwin,[2] Sara M. Haserlat,[1] Farshid Dayyani,[3] David A. Sweetser,[3] Andrea I. McClatchey,[1] Olivier A. Bernard,[4,5] A. Thomas Look,[6] Daphne W. Bell,[1] David T. Scadden,[2] and Daniel A. Haber[1]

[1]Massachusetts General Hospital Cancer Center, Boston, MA; [2]Center for Regenerative Medicine and Harvard Stem Cell Institute, Harvard Medical School, Boston, MA; [3]Department of Pediatric Hematology/Oncology, Massachusetts General Hospital, Harvard Medical School, Boston, MA; [4]Université René Descartes, Paris, France; [5]Inserm, E0210, Paris, France; and [6]Department of Pediatric Oncology, Dana-Farber Cancer Institute and Division of Hematology, Children's Hospital Boston, Harvard Medical School, MA

Ceramide is a lipid second messenger derived from the hydrolysis of sphingomyelin by sphingomyelinases (SMases) and implicated in diverse cellular responses, including growth arrest, differentiation, and apoptosis. Defects in the neutral SMase (nSMase) gene *Smpd3*, the primary regulator of ceramide biosynthesis, are responsible for developmental defects of bone; regulation of ceramide levels have been implicated in macrophage differentiation, but this pathway has not been directly implicated in human cancer. In a genomic screen for gene copy losses contributing to tumorigenesis in a mouse osteosarcoma model, we identified a somatic homozygous deletion specifically targeting *Smpd3*. Reconstitution of *SMPD3* expression in mouse tumor cells lacking the endogenous gene enhanced tumor necrosis factor (TNF)–induced reduction of cell viability. Nucleotide sequencing of the highly conserved *SMPD3* gene in a large panel of human cancers revealed mutations in 5 (5%) of 92 acute myeloid leukemias (AMLs) and 8 (6%) of 131 acute lymphoid leukemias (ALLs), but not in other tumor types. In a subset of these mutations, functional analysis indicated defects in protein stability and localization. Taken together, these observations suggest that disruption of the ceramide pathway may contribute to a subset of human leukemias. (Blood. 2008; 111:4716-4722)

Introduction

Somatic genetic alterations that arise during cancer progression may constitute incidental so-called passenger mutations, or they may be drivers of malignant proliferation, some of which may be appropriate therapeutic targets.[1] While large-scale nucleotide sequencing efforts hold the promise of comprehensive analysis of the cancer genome, initial studies have focused on known candidate cancer genes within relatively small numbers of tumors.[2-4] To complement such studies, genomic screens for gene copy number alterations have pointed to loci that may harbor recurrent abnormalities.[5,6] In fact, the initial identification of many critical tumor suppressor genes has relied on the study of rare tumors with homozygous genomic deletions targeting the relevant locus, identified by classical strategies, as well as genomic screens. These led to the discoveries of the retinoblastoma gene *RB*, the Wilms tumor suppressors *WT1* and *WTX*, the melanoma susceptibility gene *p16/INK4a*, the familial breast cancer gene *BRCA2*, and the tumor suppressor *PTEN*.[7-11]

Homozygous genomic deletions may arise by a number of mechanisms, including the overlap of 2 different allelic losses. The relatively small size of homozygous deletions, compared with much larger regions of single allelic deletions detected by loss of heterozygosity (LOH), reflects such coincidental deletion events, as well as potential selection against the homozygous loss of essential genes that may flank the relevant tumor suppressor gene. Strategies to detect gene copy losses include comparative genomic hybridization (CGH), which have resulted in the identification of novel tumor suppressors,[12,13] although the signal-noise ratio in CGH favors detection of gene amplification rather than deletion. A powerful but lower-throughput method designed specifically for identifying homozygous deletions is genomic representational difference analysis (RDA),[14] a polymerase chain reaction (PCR)–based subtractive hybridization of genomic tumor DNA from matching normal tissue. Both *PTEN*[11] and *BRCA2*[15] deletion loci were first identified using RDA. However, the extreme sensitivity of RDA, which can detect as small as 15 kb (W.J.K. and D.A.H., unpublished data, April, 2003), complicates its application to primary human cancers, since it routinely detects polymorphic deletions, which are now known to be common in the human genome.[16] To maximize the success of RDA screening for homozygous deletions associated with tumorigenesis, we adapted this strategy to analyze cell lines derived from syngeneic mouse tumor models.[17] Mouse tumors initiated by loss of *TP53* constitute a particularly interesting model, since their genomic instability may favor chromosomal events over point mutations during progression of tumorigenesis. As such, any initial discovery of candidate tumor progression genes in this model may provide clues to novel modifiers in a variety of human cancers.[17]

Submitted October 2, 2007; accepted February 3, 2008. Prepublished online as *Blood* First Edition paper, February 25, 2008; DOI 10.1182/blood-2007-10-113068.

The online version of this article contains a data supplement.

The publication costs of this article were defrayed in part by page charge payment. Therefore, and solely to indicate this fact, this article is hereby marked "advertisement" in accordance with 18 USC section 1734.

Ceramide is a lipid second messenger that triggers signal transduction pathways in response to cytokines or extrinsic cellular stresses, leading to a variety of cellular responses, including growth suppression and apoptosis.[18] Ceramide may be synthesized de novo or generated from the hydrolysis of sphingomyelin by sphingomyelinases (SMases). The pleiotrophic effect of ceramide-dependent signaling has been attributed to distinct pools of ceramide generated by different catalytic enzymes at different cellular loci.[19] To date, 4 SMases have been identified. *SMPD1* encodes lysosomal acidic SMase (aSMase), whose deficiency is associated with the autosomal recessive disorder Niemann-Pick disease.[20] A total of 3 neutral SMases (nSMases)—SMPD-2, SMPD-3, and SMPD-4—are localized to different cellular compartments and expressed in different tissues.[21-23] SMPD2 is localized to the endoplasmic reticulum (ER) and expressed in all cell types, but the mouse knockout has no phenotype.[24] SMPD4 is localized to the ER as well as to the Golgi, and has been shown to be activated in response to tumor necrosis factor α (TNFα), although its physiologic role has yet to be defined.[23] In contrast to these 2 nSMase genes, *Smpd3*-null mice have significant developmental defects, including dwarfism and delayed puberty, attributed to hypothalamic pituitary deficiency,[25] and a naturally occurring mouse model of noncollagenous osteogenesis imperfecta (fro/fro), associated with skeletal deformities and fractures, results from inactivation of *Smpd3*.[26] *SMPD3* is expressed at highest levels in the brain, is activated by TNFα, and contributes to TNFα-induced apoptosis in cultured cells.[27-29]

Here, we identified a gene-specific homozygous deletion of *Smpd3* in a mouse *TP53*-driven osteosarcoma by RDA, and extended this analysis to a panel of human tumors, demonstrating missense mutations of *SMPD3* in human leukemias. These observations raise the possibility that the ceramide pathway may be directly implicated in a subset of human cancers.

Methods

Cell lines and culture conditions

Mouse osteosarcoma cell lines derived from *TP53* heterozygous mice[30,31] and MDCK cells were maintained in Dulbecco modified Eagle medium supplemented with 10% fetal bovine serum and 1% penicillin/streptomycin at 37°C in a humidified 5% CO_2 incubator. Transient transfection of *SMPD3* expression constructs was performed using Lipofectamine 2000 reagent (Invitrogen, Carlsbad, CA) according to the manufacturer's instruction. Retroviral transduction of *SMPD3* expression constructs into adherent F4328 cells was modified from a previously described method for suspension culture.[32]

RDA and genomic deletion mapping

RDA of F4328 mouse osteosarcoma cell line was carried out as described previously.[17] For genomic Southern blot, genomic DNA was digested by *Bam*HI (New England Biolabs, Ipswich, MA), transferred onto nitrocellulose membrane (GE Healthcare, Little Chalfont, United Kingdom) and probed by radiolabeled RDA fragments cloned and excised from the pCR2.1 plasmid (Invitrogen). Primers for genomic PCR were designed from the sequences in the mouse chromosome 8 genomic contig NT 039467 (National Center for Biotechnology Information [NCBI]) and listed in Table S1A (available on the *Blood* website; see the Supplemental Materials link at the top of the online article).

Cell proliferation and viability assays

For determination of cellular proliferation, cells were plated in 96-well tissue-culture plate, grown, and fixed at appropriate time points by 4% paraformaldehyde in phosphate-buffered saline (PBS). All plates were stained by SYTO60 dye (Molecular Probes, Eugene, OR) simultaneously and quantitated using the Odyssey Imaging System (LI-COR, Lincoln, NE). TNFα-mediated cell viability was measured by MTS assay. In brief, cells in 96-well tissue-culture plates were treated with appropriate concentration of recombinant mouse TNFα (Pierce Endogen, Rockford, IL). After 4 days of incubation, 10 μL MTS solution (Promega, Madison, WI) was added to each well and incubated for 2 hours to develop color. The absorbance was measured spectrophotometrically at a wavelength of 490 nm.

Mutation analysis of *SMPD3* in human cancer cell lines and primary tumor samples

All coding exons of *SMPD3* were amplified by genomic PCR from a panel of 67 sporadic human cancer cell lines, including lung (NCI-H460, NCI-522, HOP92, NCI-15C2, NCI-1734, NCI-446, NCI-H128, NCI-H596, and NCI-H2009), ovarian (ES-2, IGROV-1, MDAH2774, OV1063, OVCAR3, OVCAR4, OVCAR5, OVCAR8, SKOV3, and SW626), brain (SF-295, SNB-19, U-251, CCF-STTG1, SW-1088, SW1783, T98G, MO59K, SK-N-DZ, and SK-N-MC), leukemia (CCRF-CEM, MOLT-4, SR, K562, and RPMI8226), prostate (DU-145 and PC-3), colon (COLO-205, HCT-116, HCT-15, HT29, and SW-620), renal (786-O, ACHN, CAKI-1, SN-12C, and UO-31), skin (LOX-IMV1, M14, and SKMEL2), bone (SAOS-2), and breast (BT549, BT483, HS157, UACC893, HS467T, HS496T, HS578T, MCF7, MDAMB175, MDAMB231, MDAMB415, MDAMB436, MDAMB 453, MDAMB468, T47D, BR-412, and MCF7ADR) cancers. For mutation screening of *SMPD3* from leukemia samples, genomic DNA from 92 primary acute myeloid leukemia (AML; 43 from Massachusetts General Hospital [MGH] and 49 from Inserm), 95 primary acute lymphoblastic leukemia (ALL), and 33 T-cell ALL (T-ALL) cell lines (ALLSIL, BE13, CCRFHSB2, CMLT1, DND41, EOL1, HBPALL, JMJURKAT, K3P, KARPAS45, KE37, KGI, KOPTK1, LOUCY, Mk-B1, MOLT-13, MOLT-15, MOLT-16, MV411, P12ICHIKAWA, PEER, PF382, REH, REX, SKM, SL-W3, SUPT1, SUPT11, SUPT13, SUPT7, TA527, TALL1, and THP; Dana-Farber Cancer Institute, Boston, MA) were collected and analyzed by genomic sequencing. Epstein-Barr virus (EBV)–immortalized lymphoblastoid cell lines established from 170 healthy blood donors provided for normal population controls. PCR primers for exon amplification and nucleotide sequencing are listed in Table S1B.

Expression constructs and site-directed mutagenesis

The coding sequence of human *SMPD3* was amplified by PCR from cDNA and cloned into pcDNA6/V5-HIS or pcDNA4/Flag (Invitrogen) or Flag-tag version of MSV-SV-GFP[32] plasmids to generate cytomegalovirus (CMV) promoter- or retrovirus-driven expression constructs, respectively. Both V5 and Flag tags were located at the C-terminus of *SMPD3*. To generate *SMPD3* mutant alleles, PCR mutagenesis was used as described.[33]

nSMase activity assay

F4328 cells were disrupted by repeated freezing and thawing in lysis buffer (25 mM Tris-Cl [pH 7.4], 5 mM EDTA, 10 mM DTT, and protease inhibitor cocktail [Roche, Indianapolis, IN]). Crude membrane fractions were sedimented by centrifugation for 2 minutes at 2500*g* and extracted with lysis buffer containing 0.2% Triton X-100. After centrifugation, 10 μg of supernatants were incubated with 20 nM [*choline-methyl*-^{14}C] sphingomyelin (PerkinElmer, Waltham, MA) for 30 minutes at 37°C in 100 μL of 100 mM Tris-Cl (pH 7.4), 10 mM $MgCl_2$, 0.2% Triton X-100, and 10 mM dithiothreitol. Reactions were terminated by the addition of 1 mL chloroform/methanol (2:1), and the aqueous phase was separated by the addition of 200 μL water. The radioactivity of the upper phase containing phosphorylcholine was measured using a liquid scintillation counter.

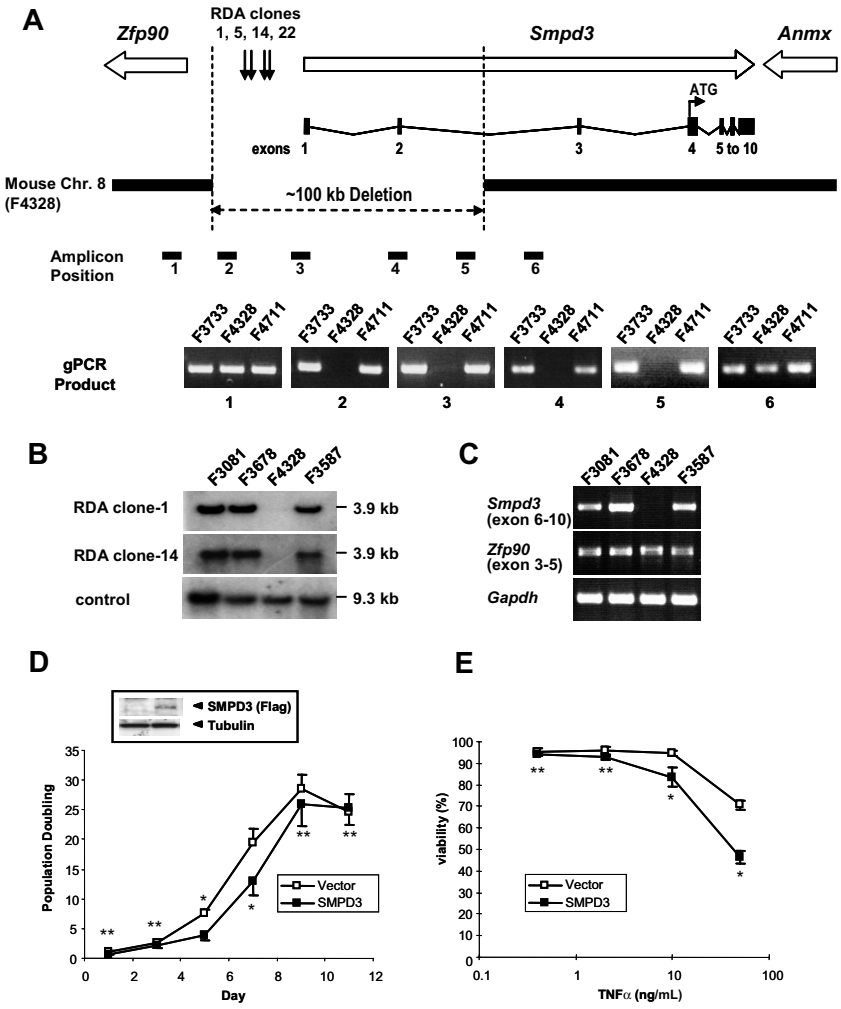

Figure 1. RDA isolation of homozygous genomic deletion at the *Smpd3* locus in F4328 mouse osteosarcoma cells. (A) Schematic representation of the homozygous deletion of the mouse chromosome 8 locus in F4328. A total of 4 nonredundant RDA clones (-1, -5, -14, and -22 [arrow])—were found in the intergenic region between *Zfp90* and *Smpd3*. Genomic PCR analysis of the first exon of *Zfp90* (1), intergenic region (2), the first (3) and the second (3) exons, and the second intron (4 and 5) of *Smpd3* in the F4328 and unrelated control F3733 and F4711 cell lines are shown. (B) Mouse genomic DNAs from F4328 and control F3081, F3678, and F3587 cell lines were digested by *Bam*HI and subjected to Southern blot analysis using RDA clone-1 or -14 as probes. A DNA fragment that was isolated by RDA due to a *Bgl*II polymorphism served as a probe for the loading control. (C) Expression of *Smpd3* and *Zfp90* genes in the F4328 cell line was analyzed by RT-PCR analysis. Primers were chosen in exons 6 and 10 for *Smpd3*, which are outside the genomic deletion. *Gapdh* was used as an internal loading control. (D,E) Reconstitution of F4328 cell lines with *SMPD3*. *SMPD3* (□) or empty vector control (■) constructs were retrovirally transduced into F4328 cells. (D) The resulting cells were plated in 96-well format for measurement of growth rate. Cell numbers were measured by the absorbance at 600 nm after staining with DNA staining dye CYTO60 and plotted as fold increase compared with day 1. Error bar indicates standard error of mean. Protein expression of SMPD3, detected by anti-Flag antibody, is shown in the inset. (E) Cells in 96-well plate format were treated with the indicated concentration of TNFα for 4 days, and cell viability was measured by MTS assay. Percentage of viability is plotted compared with the mock-treated cells. Statistical significance of each matching data point was calculated (*$P < .001$; **$P > .05$).

Cycloheximde treatment

F4328 cells in a 6-well plate format were transfected with 1 μg V5-tagged wild-type or D358G *SMPD3* in pcDNA6. At 48 hours after transfection, cells were treated with 100 μg/mL cycloheximide for various times, and total cell lysates were prepared for Western blot analysis.

Indirect immunofluorescence microscopy

MDCK cells grown on coverslips were transiently transfected with either Flag- or V5-tagged *SMPD3* or mutant *SMPD3* in pcDNA vector using Lipofectamine 2000 (Invitrogen). After 48 hours, cells were fixed with 4% paraformaldehyde in PBS for 10 minutes, permeabilized with 0.5% Triton X-100 in PBS for 10 minutes, and blocked with blocking solution (5% goat serum, 5% horse serum, 0.2% fish gelatin, and 0.2% Tween 20 in PBS) for 30 minutes at 37°C. Cells were then incubated with anti-V5 (1:250) or anti-Flag (1:250) monoclonal antibodies in blocking solution for 1 hour at 37°C, washed, probed with anti-mouse Alexa 488 (1:500; Invitrogen), washed and mounted with DAPI. A Nikon Eclipse 90i fluorescence microscope (Nikon, Melville, NY) was used for visualization of staining. NIS-Element AR 2.30 software (Nikon) was used for the acquisition of images.

Antibodies

Anti-V5, anti-Flag, and antitubulin antibodies were purchased from Invitrogen, Sigma-Aldrich (St Louis, MO), and Santa Cruz Biotechnology (Santa Cruz, CA), respectively.

Results and discussion

Homozygous deletion of *Smpd3* in a mouse osteosarcoma initiated by loss of *TP53*

We undertook an RDA screen of 3 osteosarcoma cell lines derived from mouse tumors with a heterozygous germ-line *TP53* deletion.[30] No homozygous deletions were identified in 2 cell lines, while the third (F4328) harbored homozygous deletions at a number of loci, including the known tumor suppressor gene *PTEN*. Of 4 deletion loci that did not harbor a known tumor suppressor, we selected a small homozygous deletion on chromosome 8q for detailed analysis. The chromosome 8q deletion produced 4 nonredundant RDA fragments (Figure 1A), which were used to confirm the homozygous deletion by genomic Southern blot (Figure 1B). Based on the sequence of mouse chromosome 8 genomic contig NT 039467 (NCBI), we mapped the boundary of the deletion by genomic PCR, defining a deletion of 100 kb. This gene-poor region contains the first 2 5′ exons of the *Smpd3* gene, which is localized to the centromeric border of the deletion. The coding exons of the neighboring gene *Zfp90*, which are localized at the telomeric border of the deletion, are not affected. However, since the deletion affects sequences upstream of this gene, we confirmed expression of *Zfp90* in F4328 cells by reverse transcription (RT)–PCR. In contrast, *Smpd3* expression is absent (Figure 1C).

Table 1. *SMPD3* mutations within human leukemia

Histology	Nucleotide change	Amino acid change	Frequency in controls
AML primary			
AML1	c.580G>A	Asp194Asn	0/166
AMLB5	c.580G>A	Asp194Asn	0/166
AMLB6	c.580G>A	Asp194Asn	0/166
LEUK139	c.580G>A	Asp194Asn	0/166
LEUK7	c.1519G>A	Val507Ile	0/172
ALL primary, ALL. 88-89	c.580G>A	Asp194Asn	0/166
ALL cell line			
KE37	c.127T>C	Tyr43His	0/171
	c.1073A>G	Asp358Gly	0/176
Mk-B1	c.284A>T	Tyr95Phe	0/171
	c.1073A>G	Asp358Gly	0/176
	c.1495G>C	Glu499Gly	0/174
JMJURKAT	c.151G>A	Asp51Asn	0/171
	c.742G>A	Gly248Ser	0/166
SUPT1	c.584G>A	Gly195Glu	0/166
MOLT-4	c.736C>T	Arg246Cys	0/166
SUPT11	c.1006C>T	Arg336Cys	0/166
CCRF-CEM	c.1073A>G	Asp358Gly	0/176
Polymorphisms			
Ovarian cancer			
MDAH2774	c.1850G>T	Cys617Tyr	3/43
Renal cancer			
786-O	c.1850G>T	Cys617Tyr	3/43
Myeloma			
RPMI8226	c.391C>G	Val131Leu	0/171

To test for functional consequences of the *Smpd3* deletion in F4328 cells, we reconstituted human *SMPD3* expression in these cells using retroviral infection with a bicistronic green fluorescent protein (GFP)–linked vector, allowing monitoring of infected cells by flow cytometry. The more than 80% infection rate allowed analysis of pooled infected F4328 cells, avoiding clonal selection bias. *SMPD3*-reconstituted cells displayed a modest suppression of proliferation (Figure 1D) and showed no obvious difference in contact inhibition-induced growth arrest (data not shown). However, cell viability following treatment with TNFα was significantly decreased in *SMPD3*-reconstituted cells compared with parental F4328 cells lacking the endogenous gene (Figure 1E). While the functional consequences of restoring *SMPD3* expression and ceramide biogenesis in cancer cells with a deletion of the endogenous gene may be complex, TNFα-induced reduction of cell viability provides an initial measure of ceramide signaling.

SMPD3 mutations in human leukemias

To determine whether *SMPD3* is also targeted by mutations in human cancers, we first screened a cohort of 67 sporadic human cancer cell lines from various tissue origins, including lung, ovary, brain, leukemia, prostate, colon, renal, skin, bone, and breast by bidirectional nucleotide sequencing. A total of 2 missense mutations in *SMPD3* were identified in the leukemia cell lines CCRF-CEM (ALL) and MOLT-4 (ALL). We therefore expanded our analysis to a panel of 92 cases of primary AML, 95 cases of primary ALL samples, and 33 ALL cell lines, identifying *SMPD3* mutations in an additional 11 cases. Thus, in total, *SMPD3* mutations were present in 8 (6%) of 131 ALLs and 5 (5%) of 92 AMLs (Table 1). All mutations led to nonsynonymous missense changes. Of 7 cell lines with *SMPD3* mutations, 4 are heterozygous, and 2 are compound heterozygotes. One cell line has 3 missense mutations including one homozygous mutation (E499G). All primary leukemia specimens displayed both mutant and wild-type sequences (Figure S1), presumably due to normal cell contamination. A total of 2 *SMPD3* mutations were recurrent: D194N was present in 5 independent cases and D358G was found in 3 cases. Although remission samples from leukemia cases were not available for analysis, all mutations identified in these leukemias were absent from 170 healthy population controls (340 alleles), and from the NCBI single nucleotide polymorphism database.[34] Amino acid alignment of SMPD3 from various vertebrate animals showed that of the 11 mutations, 9 mutations occurred in amino acids that are conserved in all vertebrate animals for which SMPD3 sequence is known, while 5 of them are conserved in mammals (Figure 2). Thus, most of the SMPD3 mutations in human leukemias affect highly conserved amino acids. The overall amino acid identity in SMPD3 from these species compared with human is 91% (murine), 89% (bovis and canine), 72% (chicken), 69% (xenopus), and 56% (zebrafish). In addition, computational prediction of potential impact of an amino acid substitution on the structure and function of a human protein using the Polyphen program (http://genetics.bwh.harvard.edu/pph) resulted in 4 benign, 3 possibly damaging, and 4 probably damaging mutations that are relatively well correlated with their conservation among species (Table S2).

To study the effects of leukemia-associated mutations, we generated retroviral expression constructs of wild-type *SMPD3* and the mutant alleles. Following infection of F4328 cells, nSMase activity of cellular lysates was quantified by measuring

Figure 2. Amino acid alignment of SMPD3 from various species surrounding SMPD3 mutations. The SMPD3 amino acid sequence from mammals (*Homo sapiens*, *Mus musculus*, *Bos taurus*, and *Canis familiaris*) and other vertebrate animals (*Gallus gallus*, *Xenopus laevis*, and *Danio rerio*) are aligned using MultAlin software (http://bioinfo.genopole-toulouse.prd.fr/multalin/multalin.html). Blue and red letters indicate amino acids that are conserved within mammals and vertebrates, respectively.

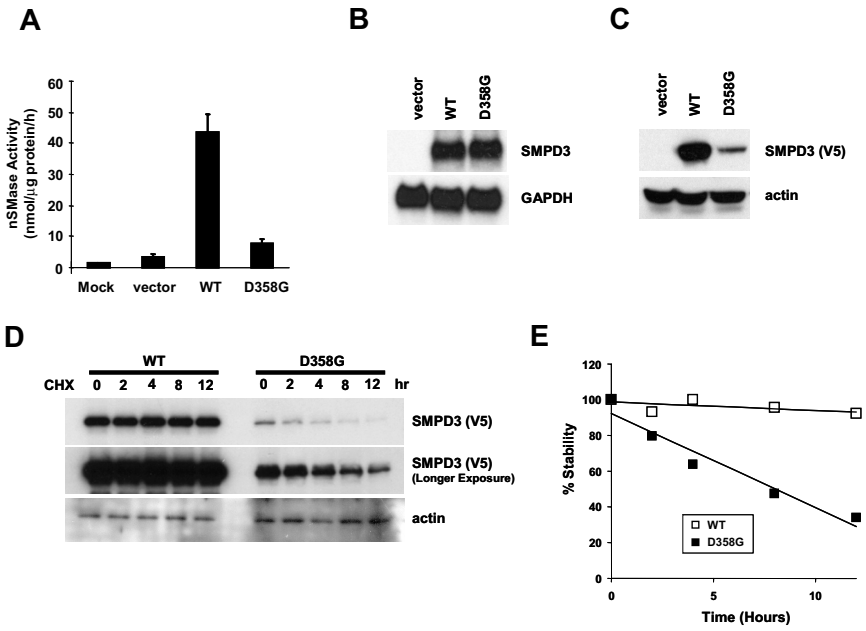

Figure 3. The D358G mutation in SMPD3 causes protein instability. (A) nSMase assay for wild-type and D358G SMPD3 lysate. Crude membrane fractions from F4328 cells expressing retrovirally transduced wild-type or D358G SMPD3 were incubated with ^{14}C-labeled sphingomyelin in the presence of the Mg^{2+} for 30 minutes at 37°C. The release of ^{14}C-phosphorylcholine in the aqueous phase was measured by scintillation counter. Error bars indicate standard error of the mean. (B,C) F4328 cells were transiently transfected with empty vector, V5-tagged wild-type, or D358G *SMPD3*. Cells were harvested 48 hours after transfection and were split for Northern (B) and Western blot analysis (C). (D) F4328 cells transiently transfected with either V5-tagged wild-type or D358G *SMPD3* were treated with 100 μg/mL cycloheximide for the indicated times, and the total cell lysates were prepared for Western blot by anti-V5 antibody. The middle panel shows a longer exposure of the same blot. (E) Western blot results were quantitated by QuantityOne software (Bio-Rad, Hercules, CA) and protein stability was plotted by percentage of the intensity of band compared with that of the untreated sample. □ indicates wild-type SMPD3; ■, D358G SMPD3.

hydrolysis of sphingomyelin into phosphorylcholine and ceramide. nSMase activity was minimal in parental F4328 cells, indicating that SMPD3 is the primary contributor to sphingomyelin hydrolysis activity in these cells. As expected, cells infected with wild-type construct had increased nSMase activity that was appropriately restricted to the crude membrane fraction, with minimal enzymatic activity in cytosolic fractions. Cells infected with the various *SMPD3* mutants showed no gross defect in nSMase activity with the exception of the recurrent mutation D358G, which showed no increase in enzymatic activity compared with the empty vector control. (Figure 3A). While similar infection rates were observed for each construct by flow cytometry, Western blot analysis showed strikingly decreased protein expression of D358G SMPD3. The consistently low levels of D358G mutant expression raised the possibility of an inherently unstable protein. Indeed, transient transfection of a CMV-driven construct into F4328 cells showed comparable levels of RNA expression for wild-type and the D358G mutant, but a marked reduction in D358G protein expression (Figure 3B,C). To determine whether the D358G mutation leads to SMPD3 protein instability, we compared the half-life of wild-type and mutant proteins by measuring protein levels following treatment with cycloheximide to block new protein synthesis. Whereas protein turnover, as measured by cycloheximide/Western blot analysis, was undetectable for wild-type SMPD3 ($t_{1/2}$ over 12 hours), the half-life of the D358G mutant was as short as 8 hours (Figure 3D,E). Thus, the recurrent D358G mutation appears to encode a grossly unstable SMPD3 protein.

Biochemical activity for nSMase has been observed primarily in the plasma membrane, and relocalization of SMPD3 from Golgi to the plasma membrane has been observed upon its activation by contact inhibition in MCF7 cells,[27] by oxidative stress in lung epithelial cells,[35] and at baseline in Hep-G2 cells.[36] To further analyze functional defects of SMPD3 mutants, we determined the subcellular localization of SMPD3 and each mutant form in the well-characterized MDCK kidney epithelial cell line. SMPD3 was localized to the plasma membrane in confluent MDCK cells (Figure 4D). Of the 11 mutants tested, 2 SMPD3 mutants, D358G and G248S, failed to localize to the plasma membrane under these conditions, showing diffuse staining throughout the cytoplasm (Figure 4G,J).

Concluding remarks

We have demonstrated that a subset of human leukemias have mutations in the nSMase gene *SMPD3*, which encode the major catalytic enzyme responsible for the generation of ceramide in response to various cellular stresses. Of the 11 mutations identified, 2 mutations showed gross defects in either protein stability and/or subcellular localization. The functional significance of the other 9 mutations is uncertain, and may require more physiologic analyses of hematopoietic differentiation. Matched normal tissues or remission specimens are not available for analysis, a common problem in mutational studies in leukemia, and we therefore cannot exclude the possibility that at least some of the other *SMPD3* variants represent rare germ-line mutations. However, their identification as likely somatic mutations is supported by their absence in large number of population controls, the absence of *SMPD3* mutations in other tumor types analyzed, and the fact that most mutations affect highly conserved residues across a different evolutionary species. Distinguishing true "driver" versus "passenger" mutations in human cancers may require detailed functional studies, as recently demonstrated in an analysis of FLT3 mutations in leukemia.[37] Consistent with that study, the presence of clearly defective *SMPD3* alleles in a subset of leukemias supports that other *SMPD3* mutations may have more moderate effects that are less readily defined in vitro. Together, these observations point to the ceramide pathway as being targeted by mutations in human leukemias.

Ceramide has been proposed as an antioncogenic lipid second messenger in multiple cancer types, where decreased levels of ceramide or increased levels of the counterbalancing sphingolipid sphingosine-1-phosphate or its metabolic enzyme sphingosine kinase 1 have been observed in cancers (reviewed in Ogretmen and Hannun[38]). However, genetic evidence supporting a specific role of the ceramide pathway in human cancer has been lacking. It is of interest that the sphingomyelin cycle was first discovered in HL-60

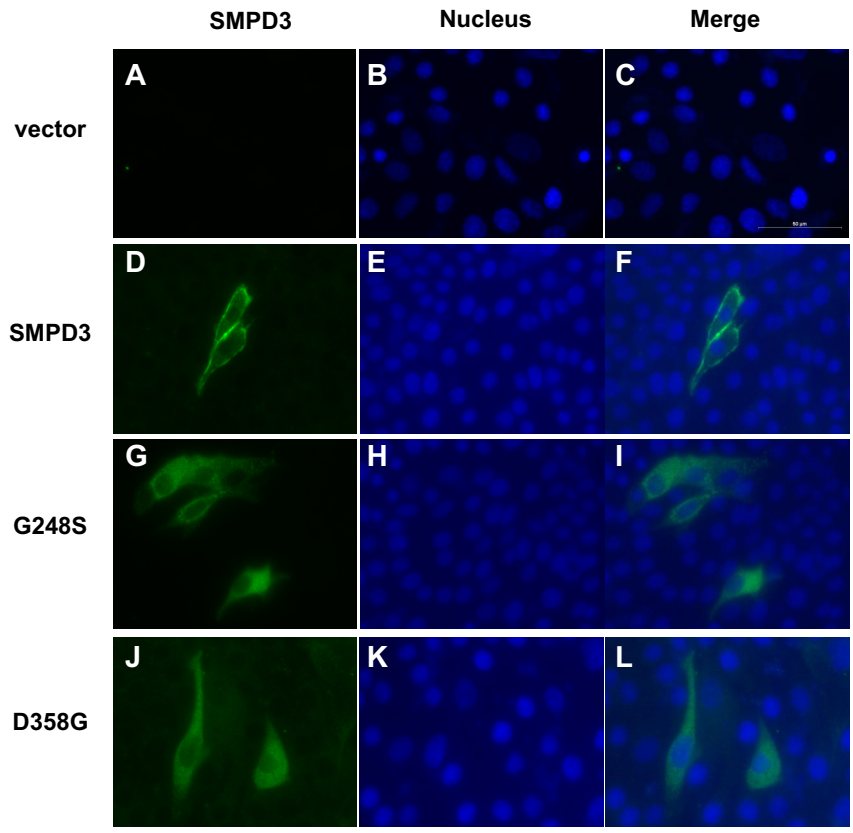

Figure 4. Subcellular localization of wild-type and mutant SMPD3 in MDCK cells. Tagged version of wild-type and mutant SMPD3 (G247S and D358G) were transfected, and their subcellular localization was determined by indirect fluorescence microscopy. More than 70% of stained cells within each sample showed similar staining as depicted in the panels. Magnification: 20×/0.75 NA Plan Apo objective of samples in Vectashield mounting medium for dluorescence with DAPI, H-1200 (Vector Laboratories, Burlingame, CA) stained with Alexa Fluor 488 goat antimouse IgG H+L (Invitrogen). Images were acquired using a Retiga 200R digital camera (QImaging, Surrey, BC) and HIS-Elements Ar 2.30 software (Nikon) and processed using Adobe Photoshop 7.0 (Adobe Systems, San Jose, CA).

human myelocytic leukemia cells, where induction of differentiation along the monocytic lineage using vitamin D_3, TNFα, and γ-interferon, but not along other lineages, activates cellular nSMase, triggering sphingomyelin hydrolysis and ceramide accumulation.[19,39-41] Thus, ceramide metabolism may play a particularly important role in hematopoetic differentiation, and its dysregulation may contribute to a subset of human leukemias. In addition to the point mutations observed here, we note the chromosomal localization of *SMPD3* on chromosome band 16q22.1, a locus rich in leukemia-associated chromosomal abnormalities.[42-44] Taken together, the finding that a significant subset of human leukemias harbors mutations in *SMPD3* provides the first genetic evidence for alterations in ceramide metabolism in human cancers.

Acknowledgments

We are grateful to Drs D. Gary Gilliland, Vijay Yajnik, Charles Paulding, and Ryn Miake-Lye for helpful discussions, reagents, and critical reading.

This work was supported by grants from the National Foundation for Cancer Research (D.A.H.), the Doris Duke Distinguished Clinical Scientist Award (D.A.H.), and the National Insitutes of Health (CA68484 and CA109901 to A.T.L.)

Authorship

Contribution: W.J.K., R.A.O., S.M.H., L.E.P., M.G., and F.D. performed experiments; A.I.M. provided mouse osteosarcoma cell lines; O.A.B., and A.T.L. provided leukemia DNA samples; W.J.K., D.A.S., D.W.B., D.T.S., and D.A.H analyzed data; W.J.K and D.A.H designed the research and wrote the paper.

Conflict-of-interest disclosure: The authors declare no competing financial interests.

Correspondence: Daniel A. Haber, Cancer Center, Massachusetts General Hospital, 149 13th St, Charlestown, MA 02129; e-mail: haber@helix.mgh.harvard.edu.

References

1. Haber DA, Settleman J. Cancer: drivers and passengers. Nature. 2007;446:145-146.
2. Bardelli A, Parsons DW, Silliman N, et al. Mutational analysis of the tyrosine kinome in colorectal cancers. Science. 2003;300:949.
3. Greenman C, Stephens P, Smith R, et al. Patterns of somatic mutation in human cancer genomes. Nature. 2007;446:153-158.
4. Sjoblom T, Jones S, Wood LD, et al. The consensus coding sequences of human breast and colorectal cancers. Science. 2006;314:268-274.
5. Maser RS, Choudhury B, Campbell PJ, et al. Chromosomally unstable mouse tumours have genomic alterations similar to diverse human cancers. Nature. 2007;447:966-971.
6. Zender L, Spector MS, Xue W, et al. Identification and validation of oncogenes in liver cancer using an integrative oncogenomic approach. Cell. 2006;125:1253-1267.
7. Lee WH, Bookstein R, Hong F, Young LJ, Shew JY, Lee EY. Human retinoblastoma susceptibility gene: cloning, identification, and sequence. Science. 1987;235:1394-1399.
8. Call KM, Glaser T, Ito CY, et al. Isolation and characterization of a zinc finger polypeptide gene at the human chromosome 11 Wilms' tumor locus. Cell. 1990;60:509-520.
9. Nobori T, Miura K, Wu DJ, Lois A, Takabayashi K, Carson DA. Deletions of the cyclin-dependent kinase-4 inhibitor gene in multiple human cancers. Nature. 1994;368:753-756.
10. Wooster R, Bignell G, Lancaster J, et al. Identification of the breast cancer susceptibility gene BRCA2. Nature. 1995;378:789-792.
11. Li J, Yen C, Liaw D, et al. PTEN, a putative protein tyrosine phosphatase gene mutated in human brain, breast, and prostate cancer. Science. 1997;275:1943-1947.
12. Rivera MN, Kim WJ, Wells J, et al. An X chromosome gene, WTX, is commonly inactivated in Wilms tumor. Science. 2007;315:642-645.

13. Mullighan CG, Goorha S, Radtke I, et al, Downing JR. Genome-wide analysis of genetic alterations in acute lymphoblastic leukaemia. Nature. 2007; 446:758-764.
14. Lisitsyn N, Wigler M. Cloning the differences between two complex genomes. Science. 1993;259:946-951.
15. Schutte M, da Costa LT, Hahn SA, et al. Identification by representational difference analysis of a homozygous deletion in pancreatic carcinoma that lies within the BRCA2 region. Proc Natl Acad Sci U S A. 1995;92:5950-5954.
16. Iafrate AJ, Feuk L, Rivera MN, et al. Detection of large-scale variation in the human genome. Nat Genet. 2004;36:949-951.
17. Yajnik V, Paulding C, Sordella R, et al. DOCK4, a GTPase activator, is disrupted during tumorigenesis. Cell. 2003;112:673-684.
18. Hannun YA. Functions of ceramide in coordinating cellular responses to stress. Science. 1996; 274:1855-1859.
19. Levade T, Jaffrezou JP. Signalling sphingomyelinases: which, where, how and why? Biochim Biophys Acta. 1999;1438:1-17.
20. Schuchman EH, Suchi M, Takahashi T, Sandhoff K, Desnick RJ. Human acid sphingomyelinase: isolation, nucleotide sequence and expression of the full-length and alternatively spliced cDNAs. J Biol Chem. 1991;266:8531-8539.
21. Tomiuk S, Hofmann K, Nix M, Zumbansen M, Stoffel W. Cloned mammalian neutral sphingomyelinase: functions in sphingolipid signaling? Proc Natl Acad Sci U S A. 1998;95:3638-3643.
22. Hofmann K, Tomiuk S, Wolff G, Stoffel W. Cloning and characterization of the mammalian brain-specific, Mg2+-dependent neutral sphingomyelinase. Proc Natl Acad Sci U S A. 2000;97:5895-5900.
23. Krut O, Wiegmann K, Kashkar H, Yazdanpanah B, Kronke M. Novel tumor necrosis factor-responsive mammalian neutral sphingomyelinase-3 is a C-tail-anchored protein. J Biol Chem. 2006;281:13784-13793.
24. Zumbansen M, Stoffel W. Neutral sphingomyelinase 1 deficiency in the mouse causes no lipid storage disease. Mol Cell Biol. 2002;22:3633-3638.
25. Stoffel W, Jenke B, Block B, Zumbansen M, Koebke J. Neutral sphingomyelinase 2 (smpd3) in the control of postnatal growth and development. Proc Natl Acad Sci U S A. 2005;102:4554-4559.
26. Aubin I, Adams CP, Opsahl S, et al. A deletion in the gene encoding sphingomyelin phosphodiesterase 3 (Smpd3) results in osteogenesis and dentinogenesis imperfecta in the mouse. Nat Genet. 2005;37:803-805.
27. Marchesini N, Osta W, Bielawski J, Luberto C, Obeid LM, Hannun YA. Role for mammalian neutral sphingomyelinase 2 in confluence-induced growth arrest of MCF7 cells. J Biol Chem. 2004; 279:25101-25111.
28. Luberto C, Hassler DF, Signorelli P, et al. Inhibition of tumor necrosis factor-induced cell death in MCF7 by a novel inhibitor of neutral sphingomyelinase. J Biol Chem. 2002;277:41128-41139.
29. Clarke CJ, Truong TG, Hannun YA. Role for neutral sphingomyelinase-2 in tumor necrosis factor alpha-stimulated expression of vascular cell adhesion molecule-1 (VCAM) and intercellular adhesion molecule-1 (ICAM) in lung epithelial cells: p38 MAPK is an upstream regulator of nSMase2. J Biol Chem. 2007;282:1384-1396.
30. Jacks T, Remington L, Williams BO, et al. Tumor spectrum analysis in p53-mutant mice. Curr Biol. 1994;4:1-7.
31. McClatchey AI, Saotome I, Mercer K, et al. Mice heterozygous for a mutation at the Nf2 tumor suppressor locus develop a range of highly metastatic tumors. Genes Dev. 1998;12:1121-1133.
32. Ellisen LW, Carlesso N, Cheng T, Scadden DT, Haber DA. The Wilms tumor suppressor WT1 directs stage-specific quiescence and differentiation of human hematopoietic progenitor cells. EMBO J. 2001;20:1897-1909.
33. Higuchi R, Krummel B, Saiki RK. A general method of in vitro preparation and specific mutagenesis of DNA fragments: study of protein and DNA interactions. Nucleic Acids Res. 1988;16: 7351-7367.
34. National Center for Biotechnology Information. Single Polymorphism Nucleotide database. Available at: http://www.ncbi.nlm.nih.gov/projects/SNP/. Accessed January 22, 2008.
35. Levy M, Castillo SS, Goldkorn T. nSMase2 activation and trafficking are modulated by oxidative stress to induce apoptosis. Biochem Biophys Res Commun. 2006;344:900-905.
36. Karakashian AA, Giltiay NV, Smith GM, Nikolova-Karakashian MN. Expression of neutral sphingomyelinase-2 (NSMase-2) in primary rat hepatocytes modulates IL-beta-induced JNK activation. FASEB J. 2004;18:968-970.
37. Frohling S, Scholl C, Levine RL, et al. Identification of driver and passenger mutations of FLT3 by high-throughput DNA sequence analysis and functional assessment of candidate alleles. Cancer Cell. 2007;12:501-513.
38. Ogretmen B, Hannun YA. Biologically active sphingolipids in cancer pathogenesis and treatment. Nat Rev Cancer. 2004;4:604-616.
39. Kim MY, Linardic C, Obeid L, Hannun Y. Identification of sphingomyelin turnover as an effector mechanism for the action of tumor necrosis factor alpha and gamma-interferon: specific role in cell differentiation. J Biol Chem. 1991;266:484-489.
40. Okazaki T, Bell RM, Hannun YA. Sphingomyelin turnover induced by vitamin D3 in HL-60 cells. Role in cell differentiation. J Biol Chem. 1989; 264:19076-19080.
41. Liu B, Obeid LM, Hannun YA. Sphingomyelinases in cell regulation. Semin Cell Dev Biol. 1997;8: 311-322.
42. Betts DR, Rohatiner AZ, Evans ML, Rassam SM, Lister TA, Gibbons B. Abnormalities of chromosome 16q in myeloid malignancy: 14 new cases and a review of the literature. Leukemia. 1992;6: 1250-1256.
43. Marlton P, Keating M, Kantarjian H, et al. Cytogenetic and clinical correlates in AML patients with abnormalities of chromosome 16. Leukemia. 1995;9:965-971.
44. Hogge DE, Misawa S, Parsa NZ, Pollak A, Testa JR. Abnormalities of chromosome 16 in association with acute myelomonocytic leukemia and dysplastic bone marrow eosinophils. J Clin Oncol. 1984;2:550-557.